♦Copper (II) ions modulate Angiogenin activity in human endothelial cells

Chiara Giacomelli[1], Maria Letizia Trincavelli[1*], Cristina Satriano[2], Örjan Hansson[3], Diego La Mendola[1*], Enrico Rizzarelli[4] and Claudia Martini[1]

1 Department of Pharmacy, University of Pisa, 56126 Pisa, Italy.

2 Department of Chemical Sciences, University of Catania, Viale Andrea Doria, 6, I-95125 Catania, Italy.

3 Department of Chemistry and Molecular Biology, University of Gothenburg, PO Box 462, SE-40530 Gothenburg, Sweden.

4 Institute of Biostructures and Bioimages, National Council of Research (CNR), Viale Andrea Doria, 6, I-95125 Catania, Italy.

Corresponding authors:

Maria Letizia Trincavelli
Department of Pharmacy, University of Pisa
Via Bonanno 6, I-56126 Pisa, Italy.
Phone: +39-050-2219522
Email: maria.trincavelli@for.unipi.it

Diego La Mendola
Department of Pharmacy, University of Pisa,
Via Bonanno 6, I-56100 Pisa, Italy.
Phone: +39-050-2219533
E-mail: lamendola@farm.unipi.it

ABSTRACT:

Angiogenin (ANG), a member of the secreted ribonuclease family, is a potent angiogenesis stimulator that interacts with endothelial cells inducing a wide range of responses. Metal ions dyshomeostasis play a fundamental role in the onset of neurodegenerative diseases, in particular copper that is also involved in angiogenesis processes. It is known that vascular pathologies are present in neurodegenerative diseases and Angiogenin is down-regulated in Alzheimer and Parkinson diseases, as well as it has been found as one of the mutated genes in amyotrophic lateral sclerosis (ALS). Copper (II) induces an increase of Angiogenin binding to endothelial cells but, so far, the relationship between copper-ANG and angiogenesis induction remain unclear. Herein, the effects of copper (II) ions on Angiogenin activity and expression were evaluated. The binding of copper was demonstrated to affect the intracellular localization of protein decreasing its nuclear translocation. Moreover, the ANG-copper (II) system negatively affects the protein-induced angiogenesis, as well as endothelial cells migration. Surprisingly, copper also reveals the ability to modulate the Angiogenin transcription. These results highlight the tight relationship between copper and Angiogenin, pointing out the biological relevance of ANG-copper system in the regulation of endothelial cell function, and revealing a possible new mechanism at the basis of vascular pathologies.

Keywords: Angiogenin, Copper, Angiogenesis, Human endothelial cells, ALS.

1. Introduction

Angiogenin (ANG) is a 14.2 kDa angiogenic protein overexpressed in many types of cancers (Tello-Montoliu, 2006) as well as down-regulated in several neurodegenerative diseases including amyotrophic lateral sclerosis (ALS) (Aparicio-Erriu and Prehn, 2012), Parkinson's disease (PD) (Steidinger, 2011) and Alzheimer's disease (AD)(Kim and Kim, 2012). Furthermore, loss-of-function mutation of ANG has been related to the onset of PD and ALS (Crabtree, 2007; Greenway, 2006; Padhi, 2012; Steidinger, 2011; Wu, 2007). The onset and progression of neurodegenerative disease have been related for long time to the accumulation of insoluble misfolded protein such as β-amyloid (Cavallucci, 2012; Hardy and Higgins, 1992) and, more recently, to alteration of metallostasis (metal dys-homeostasis) (Ayton, 2013; Milardi and Rizzarelli, 2011; Tiiman, 2013) as well as to the neurovascular abnormalities (Chen, 2013; Drachman, 2014; Lyros, 2014). Thus, the understanding of the link between metal ions, angiogenic proteins and angiogenesis may be helpful to develop new therapeutic strategies concerning of cancer and neurodegenerative disease such as AD and ALS.

ANG plays a crucial role as stress-regulator balancing cell growth and survival depending on cellular status (Del Giudice, 2014; Li and Hu, 2012). Under growth conditions, ANG is rapidly translocated into the nucleus of cancer cells (Yoshioka, 2006), motoneurons (Kieran, 2008; Subramanian, 2007) and endothelial cells (Hu, 2000; Li, 1997) and promotes the ribosomal RNA (rRNA) transcription (Sheng, 2014). Under stress conditions, ANG relocates into the cytoplasm where it is accumulated in stress granules (SGs) and mediates the production of stress-induced tRNA-derived ~40 nucleotide non coding RNAs (designated as 3′-tiRNAs) (Pizzo, 2013; Yamasaki, 2009).

ANG interacts with endothelial and smooth muscle cells inducing a wide range of effects including cell migration (Hu, 1994; Wei, 2011), invasion (Hu, 1994), proliferation (Hu, 1997, 1998a; Sadagopan, 2009), and tube formation (Miyake, 2014). The nuclear translocation, ribonucleolytic activity and signalling transduction of ANG are needed to maintain its angiogenic activity (Gao and Xu, 2008).

Interestingly, divalent copper increases the apparent number of ANG molecules bound to endothelial cells even if the apparent dissociation constant remains unchanged (Badet, 1989; Soncin, 1997a). However, other data suggested that ANG and Copper act through different mechanisms in regulating angiogenesis (Hu, 1998a). Copper is one of the most abundant transition metal in the body and it is essential for multiple biological pathways (Peña, 1999). Copper is a well-known angiogenic factor *in vivo* even though the molecular and cellular mechanism by which this action takes place is still unclear (D'Andrea, 2010). Copper dyshomeostasis has been also related to

the onset and progression of neurodegenerative diseases (Iakovidis, 2011; Noda, 2013; Park, 2014). Thus, the metal ion interaction with angiogenic factor such as ANG could be part of the mechanism and/or angiogenic signalling of copper. In this context, a more detailed characterization of ANG-copper interaction could represent a valuable aid in a better understanding of potential mutual biological influences.

Soncin et al. (1997a) have reported that the recombinant ANG tightly binds about 2.4 copper ions per molecule at physiological pH. It has been shown that ANG binds copper ion, involving preferentially the ribonucleolytic site and/or the putative receptor binding site of the protein (La Mendola, 2010, 2012). Herein, we investigated the influence of copper binding to ANG on the properties and functions of the protein in endothelial cells. Copper reduces the ribonucleolytic and angiogenic activity of ANG. Furthermore, in endothelial cells, copper favours the cytosolic localization of ANG without effects on the proliferative and survival activity of the protein. Although the exact mechanism has to be discovered, these results pointed out a tight relation of ANG and copper.

2. Materials and methods

2.1 Material

Human umbilical vein endothelial cells (HUVECs) and cell culture medium (EGM®-2 BulletKit®) were purchased from Lonza srl (Milan, Italy). All other reagents were obtained from standard commercial sources and were of the highest commercially available grade.

2.2 Protein Expression of ANG and its mutants

Expression of recombinant human ANG was carried out following a previously reported method (Holloway, 2001). The protein was refolded from inclusion bodies according to the procedure developed by Jang et al. (2004). Conversion of Met-(-1) ANG to the authentic <Glu-1 protein was achieved as described in supplementary data. The H114Y mutant was generated using the Quikchange Site-Directed mutagenesis kit according to manufacturer's instructions (Supplementary data).

2.3 Ribonucleolytic Activity

The ribonucleolytic activity toward tRNA was determined by measuring the formation of perchloric acid-soluble fragments as reported (La Mendola, 2012). Briefly, ANG (0.5 µM) and tRNA (2 mg/mL) were incubated at pH 7.4 (33 mM MOPS, 33 mM NaCl) in the presence or absence of $CuSO_4$ (0-15 µM). After 2 h at 37 °C, the solution (300 µL) was diluted with ice-cold 3.4% $HClO_4$ (700 µL) and kept on ice for 10 min. Finally, the sample was centrifuged (10000 x g) for 10 min and the absorbance of perchloric acid soluble fragments was measured at 260 nm.

2.4 Cell Lines and Drug Treatments

HUVECs were maintained in EGM®-2 BulletKit® medium. Cells were grown at 37 °C in a humid atmosphere in the presence of 5% CO_2. HUVECs were grown to 80% confluence and used in successive experiments until the sixth detaching passage. When ANG was used in combination with copper, in order to allow the formation of the complex, ANG and copper was combined 2 hours prior the cells treatment.

2.5 ERK 1/2 phosphorylation assays

HUVECs were seeded in 96-well plates at a density of $5x10^3$ cells/well for 24h in EGM®-2 medium. Cells were starved for 12 h before the experiment using EBM®-2 medium and were treated with various concentration of ANG in the presence or absence of $CuSO_4$ for different times (0-60 min). Then, the ERK 1/2 phosphorylation and the total ERK 1/2 were evaluated as previously described (Wong, 2004) with few modification (for detailed see Supplementary data). In parallel, a

western blot analysis of total ERK1/2 and phosphor-ERK1/2 was performed as previously described (Schafe, 2008) with few modifications (Supplementary data). The primary antibodies used were anti-GAPDH (G9545 Sigma-Aldrich), anti-phospho ERK1/2 (sc-7383 SantaCruz) and anti-ERK1/2 (#4695 Cell Signaling Technology). The secondary antibodies were goat anti-rabbit IgG-HRP (12-348 Millipore) and goat anti-mouse IgG-HRP (12-349 Millipore).

2.6 ANG and 45S rRNA expression levels

In order to evaluate the 45S rRNA and ANG mRNA expression a real-time RT-PCR was performed as previously described (Nolan, 2006). Briefly, HUVECs were treated with ANG or $CuSO_4$ alone or in combination in growth medium. Total RNA was extracted using the RNeasy® Mini Kit (Quiagen) according to manufacturer's instructions, and the real-time RT-PCR reactions was performed (Supplementary data). mRNA levels for each sample were normalised against β-actin mRNA levels, and relative expression was calculated using the Ct value.

2.7 Immunofluorescence and confocal microscopy

HUVEC cells were cultured on coverslips at $2x10^4$ cell/cm^2 in EGM®-2 and treated with ANG (100 nM) in the presence or absence of $CuSO_4$ (100 nM- 500 nM) for different times (5-60 min). The antibodies used were anti-ANG (0.4 µg/ml, dil. 1:500, sc-9044 Santa-Cruz) and Alexa-Fluor-488-conjugated goat anti-rabbit (2 µg/ml, dil. 1:1000, A11008 Life Technologies). Non-specific binding was controlled by omitting the primary antibody or by substituting the same concentration of non specific isotypic immunoglobulin (Data not shown). Nuclei were stained with DAPI (1:5000 diluition; Sigma-Aldrich). Confocal microscopy was performed with an Olympus FV1000 confocal laser scanning microscope (LSM) equipped UV/visible lasers: 405 nm (50 mW), 20 mW Multiline Argon laser (457 nm, 488 nm, 515 nm, total 30 mW), HeNe(G) laser (543 nm, 1 mW), HeNe(R) laser (633 nm, 1 mW); oil immersion objective (60xO PLAPO) and spectral filtering system. Emitted light was detected in sequential mode. Acquisition parameters were: 405 nm excitation at 12% laser power, emission filter SDM490 (band pass) 425–475 nm, PMT voltage at 530 V (channel 1, blue); 488 nm excitation at 16% laser power, emission filter SDM560, 500–600 nm, PMT voltage at 695 V (channel 2, green). The detector gain was fixed at a constant value and images were taken for all of the samples at random locations throughout the area of the well. Images analysis was carried out using Image J (version 1.46e, public domain, Image Processing and Analysis in Java, National Institutes of Health). The statistical analysis was performed with a one-way Anova test by using Microcal Origin (version 8.6).

2.8 Measurement of cell migration by in vitro scratch assay

ANG induction of migration was evaluated with a scratch assay. HUVECs were seeded in 96 well plates and grown to 90% of confluence. Then the scratch was made through the cell layer using a sterile micropipette tip. After washing with PBS, cells were treated with ANG in the presence or absence of $CuSO_4$ in growth medium. The images of the wounded area were captured immediately after the scratch (t_0) and 8h later (t_8) to monitor cell migration into the wounded area. Cells were fixed with 4% formaldehyde, stained with 0.5% Crystal violet for 20 min, and washed with water. Photographs were then taken at 10× magnification on an inverted microscope. The migration abilities were quantified by measuring both the average gap width and the percentage of gap closed. The data were analysed with the Image J software (Version 1.41o).

2.9 Tube formation assay

Matrigel (BD Bioscence) was thawed at 4°C overnight and spread evenly over each well (50 µl) of a 96-well plate. The plates were incubated for 30 min at 37°C to allow the Matrigel to gel before the cell seeding. HUVEC cells ($1x10^4$) from passage 3 or earlier were seeded in 100 µl of EGM-2 per well in the absence or presence of ANG and copper in combination or alone. After 16h of incubation at 37°C, the tube structures were observed with an inverted microscope equipped with a digital camera (Nikon, Sesto Fiorentino, Italy). Two fields (magnification 4×) were captured for each sample, performed in triplicate. For each image, the total length of the tube network, the number of intact loops and the number of branching points were quantified with the image analysis software ImageJ using the plug-in AngioJ for the angiogenesis assay.

2.10 Cell viability assay (MTS)

The MTS assay was performed to compare the viability of cells treated with different concentration of ANG and $CuSO_4$ alone or in combination. The cells were seeded in 96-well plates ($1.5×10^3$ cell/well for proliferation; $5x10^3$ cell/well for survival). Cells were treated with growth media or serum-free media for different times. In parallel, the control without the cells (blank) was prepared. For the MTS assay, the CellTiter 96® AQueous One Solution Cell Proliferation Assay kit (Promega) was used following the manufacturer's instruction. The blank was subtracted from the absorbance of each treatment. Then, the results were reported as the percentage versus the control set to 100%.

2.11 siRNA mediated inhibition of gene expression in transfected cells

HUVEC cells were transfected with a siRNA specifically designed for the silencing of the human ANG (sc-39291 SantaCruz). The siRNAs have been transfected with siRNA transfection reagent (Santa Cruz Biotecnology) to a final concentration of 50 nM, following the manufacturer's

protocol. In parallel to each silencing experiment, an ineffective sequence of RNA has been used as negative control (Santa Cruz Biotechnology). The silence efficacy was verified by RT-PCR. The RT-PCR products were visualized after electrophoresis migration in a 2% agarose gel and stained with ethidium bromide. Fragment sizes were confirmed by comparison with a 100 pb DNA ladder molecular weight marker (Promega). The bands were viewed under UV light and analyzed by densitometric analysis using the ImageJ (ImageJ Software, version 1.41o). Transfected cells were used 24 h after siRNA transfection.

2.12 Statistical Analysis

A non-linear multipurpose curve-fitting program, Graph-Pad Prism (Version 5.00), was used for data analysis and graphic presentation. Data were reported as the mean ± SEM of at least three different experiments. Statistical analyses were performed using a one-way ANOVA study followed by the Bonferroni test for repeated measurements. Differences were considered statistically significant when $P<0.05$.

3. Results

3.1 Copper reduces ribonucleolytic activity of ANG

Copper has been shown previously to inhibit ANG ribonucleolytic activity (Lee and Vallee, 1989). Herein the influence of increasing concentration of copper on ANG (<Glu-1 ANG) activity was evaluated as previously reported for the Met-(-1) ANG (La Mendola, 2012). The production of tRNA perchloric-acid soluble fragment was measured after the addition of 1:1 to 1:30 equivalents of $CuSO_4$ (Fig. 1A). Increasing concentration of copper (II) ions caused a strong decrease of the ribonucleolytic activity of ANG, accordingly with preliminary data reported for the recombinant ANG (La Mendola, 2012). The presence of five equivalent of copper was sufficient to cause a significant decrease of the enzymatic activity (ANG 73.7±0.6%; $P<0.001$ Fig. 1A). As previously suggested for the recombinant protein, copper could preferentially bound the residues in the catalytic core, and this could explain why the presence of a small amount of copper could be sufficient to produce a significant decrease of the ribonucleolytic activity of ANG.

3.2 Copper influences ERK1/2 phosphorylation induced by ANG

ANG promotes the activation of the extracellular-signal-regulated kinases (ERKs) (Liu, 2001) that play a central role in membrane-to-nucleus communication (Yang, 2013). In order to verify the effect of copper on ANG -mediated ERK activation, the phosphorylation of ERK1/2 in HUVEC cells was evaluated. Considering that ANG binds at least one copper ion (La Mendola, 2012) and its ribonucleolytic activity was significantly decreased in the presence of 1:5 equivalent of copper, further experiments were performed in the presence of 1:1 to 1:5 ANG/$CuSO_4$ molar ratio. The temporal response pattern of ERK1/2 activation induced by ANG and copper alone was similar, in accordance with literature data (Liu, 2001; Nawaz, 2006). They presented a peak at 5 minutes and returned to basal levels after 60 min (Fig. 1B-E). Interestingly, cell treatment with the ANG-copper system caused a sustained activation of ERK. In fact after 60 minutes of treatment the presence of copper significantly increased the phosphorylated ERK 1/2 in a concentration-dependent manner (ANG 100 nM 103.9±6.9%; $CuSO_4$ 500 nM 110.9±9.7%; ANG + $CuSO_4$ 149.8±12.4%; $P<0.001$ Fig. 1C). These results were confirmed by immunoblots analysis (Fig. 1D-E). In parallel, the total ERK was measured, showing no significant difference between the treatments (Fig. 1E, S1).

3.3 Copper decreases 45S rRNA synthesis induced by ANG

ANG is rapidly translocated into the nuclei of human endothelial cells (Hu, 2000) where promotes ribosome biogenesis through the binding of 45S ribosomal DNA (rDNA) promoter and enhancing ribosomal RNA transcription (Sheng, 2014). In order to understand if copper could affect the ribosome biogenesis induced by ANG, a real-time quantification of the 45S rRNA was performed (Fig. 1F). Compared to the untreated cells, ANG caused a marked increase of 45S transcription (ANG 3.7±0.9 fold vs control; $P<0.001$). This effect was completely counteracts by Neomycin pre-treatment that is able to inhibit the ANG translocation to the nuclei (Hu, 1998b). Copper alone was also able to enhance the transcription of the 45S, an event probably related to its proliferating activity. Interestingly, the treatment with the ANG-copper system caused a significant decrease of 45S transcription ($CuSO_4$ 100 nM 2.1±0.5; $CuSO_4$ 500 nM 2.2±0.8; ANG + $CuSO_4$ 100 nM 1.9±0.3 $P<0.01$; ANG + $CuSO_4$ 500 nM 2.2±0.2 $P<0.01$ fold vs ANG; Fig. 1F).

3.4 The ANG-copper system presents a different intracellular localization versus the ANG alone

Immunofluorescence assay was performed in order to verify the effect of copper on ANG localization, (Fig. 2A-C). HUVECs visualization by confocal microscopy showed the low amount of endogenous ANG present in the control. Copper alone slightly increased the fluorescence intensity in cytoplasm showing "pool" of ANG in a similar way to that observed in stress-induced formation of stress granules (Emara, 2010; Pizzo, 2013).

As expected, the exogenous ANG was rapidly internalized and translocated almost completely into the nuclei after 60 min of treatment, in accordance with literature data (Fig. 2 A-C) (Sadagopan, 2009). Interestingly, when the ANG-copper pre-formed complex was added, ANG remained more concentrated in the cytosol or in proximity of nuclear and cellular membrane (Fig. 2A-C). These results, in accordance with previous data highlight the importance of copper binding to ANG in the regulation of its intracellular localization.

3.5 Copper modulate the ANG migration and angiogenesis activity

Considering the effect of copper on intracellular trafficking of ANG, the metal ions effect on HUVECs migration was firstly investigated. In accordance with previous data (Jimi, 1995), exogenous ANG significantly increased HUVECs migration (Ctrl 27.5±2.7%; ANG 100 nM 61.6±5.1%; $P<0.001$ vs Ctrl Fig. 3A-B). Copper at high micromolar concentration promotes the cell migration (McAuslan and Reilly, 1980). However, the sub-micromolar concentrations of copper were not able to affect cell migration that remained comparable to the control (Fig. 3A-B).

Interestingly, a decrease in cell migration in the presence of the ANG-copper system was observed (ANG 100 nM + $CuSO_4$ 100 nM 43.8±3.4% P<0.01 vs ANG; ANG100 nM + $CuSO_4$ 500 nM 24.2±3.8% P<0.001 vs ANG; Fig. 3A-B). Additionally, increasing concentration of copper caused a further decrease of cell migration.

A capillary-like tube formation assay on Matrigel (Khoo, 2011) was performed to determine whether copper could affect the angiogenic property of ANG. In untreated cells, HUVECs began at 4 h to form tube-like structures that were evident at 16 h of culture (Fig. 4A-D), in accordance with literature data (Miyake, 2014). As expected, ANG alone was able to promote angiogenesis increasing the tube length, branching points and meshes number after 4h and becoming more evident after 16h (tube length: ANG 100 nM 15384.4±383.6, P<0.01; branching points: ANG 100 nM 147.8±4.6%, P<0.01; meshes number: ANG 100 nM 225.5±13.0%, P<0.01 vs Ctrl Fig. 4A-D). Among the different features of ANG, the ribonucleolytic activity and nuclear translocation are necessary for the ANG -induced angiogenesis (Gao and Xu, 2008). The pre-treatment with Neomycin completely counteracted the angiogenic effect of ANG, in accordance with previous data (Hu, 1998b). Furthermore, the H114Y ANG mutant, that completely loss the ribonucleolytic activity (data not shown), was not able to enhance the angiogenesis process (Fig. 4A-D).

Copper alone presents angiogenic effect at high micromolar concentration (Narayanan, 2013). However, nanomolar concentrations were used so to avoid copper induction of angiogenesis (Fig. 4A-D). Noteworthy, the treatment with the ANG-copper system significantly decreased the angiogenic effect of the protein. The reduction of tube length, branching points and meshes number was evident after 4h, and became more evident after 16h of treatment (Fig. 4A-D). The inhibition of ANG ribonucleolytic activity and nuclear translocation completely abolish the angiogenesis induction. Copper alone, as demonstrated above, inhibits ANG ribonucleolytic activity (Fig. 1A) as well as decreases ANG nuclear translocation demonstrated by the inhibition of ANG -induced 45S transcription (Fig. 1F) and the increasing of cytosolic protein concentration (Fig. 2A-C). Thus, the inhibition of ANG -induced angiogenesis by copper could be due to its effects on the protein properties.

3.6 Copper modulates the ANG proliferative and pro-survival activity

In order to evaluate the proliferative and pro-survival effects of ANG, viability assays in HUVEC cells were performed. As expected, ANG was able to increase significantly the proliferation of endothelial cells in a concentration dependent manner (Fig. S2A-B). Furthermore, ANG significantly affected the human endothelial cells survival in serum-withdrawal condition, a commonly used method to induce HUVECs apoptosis (Asada, 2008; Michaelis, 2006) (Fig. S2C-

D). Thus, the effect of the ANG-copper system on HUVECs proliferation after 24h and 48h was evaluated (Fig. 5A-B). Copper alone was able to increase the proliferation, although this effect became significant only after 48h of treatment. Differently, the ANG-copper system did not significantly affect the endothelial proliferation rate after 24h and 48h of cells treatment (Fig. 5A-B).

Then, the pro-survival activity was evaluated. Results were comparable to those obtained in the proliferative assays. Copper as well as ANG alone significantly improved the survival of HUVECs (Fig. 5C). The ANG-copper system did not significantly affect the pro-survival effect versus the protein alone; conversely, survival rate appeared to be significantly higher with respect to copper alone when was used at higher concentration ($CuSO_4$ 500 nM 151.7±9.2%, $CuSO_4$ 2.5 µM 143.0±6.9%; ANG 100 nM + $CuSO_4$ 500 nM 179.7±8.2% $P<0.01$; ANG 500 nM + $CuSO_4$ 500 nM 226.7±3.6% $P<0.001$; ANG 500 nM + $CuSO_4$ 2.5 µM 195.8±7% $P<0.01$; Fig. 5C).

3.7 Copper influences the ANG expression and ANG silencing evidence the effect of ANG-copper system on HUVEC cells proliferation

Copper is known to be able to increase the gene expression of pro-angiogenic and proliferative factor such as VEGF (Sen, 2002), but to date no results have been reported about the effect of copper on the ANG gene expression. Thus, in order to explain the discrepancy of the ANG-copper system effects on angiogenesis induction and endothelial cells proliferation, the ANG mRNA expression was evaluated by real-time PCR analysis (Fig. 5D). Noteworthy, copper significantly increased the ANG transcription after 24h at the highest concentration ($CuSO_4$ 500 nM 1.6±0.2 fold, $P<0.01$ at 24 h and $CuSO_4$ 500 nM 2.9±0.4 fold; $P<0.001$ at 48 h. Fig. 5D) and become significant after 48h of treatment at both concentration ($CuSO_4$ 100 nM 1.8±0.2 fold $P<0.001$; Fig. 5D). The copper promotion of ANG transcription could partially explain the diverse effect showed by the ANG-copper system on angiogenesis and proliferation.

In order to demonstrate the effect of copper transcriptional activity on HUVECs proliferation, the ANG expression was suppressed by using random siRNA or siRNAs specifically designed to silence ANG. The efficiency of siRNA transfection in reducing ANG gene expression was demonstrated by RT-PCR (Fig. 6A-B). The proliferative activity of exogenous ANG was then evaluated. After 24h of treatments, ANG alone increased the proliferation rate, in a concentration dependent manner (30.9±6.7 nM; Fig. 6C-D). These effects became more evident after 48h of treatment (Fig. 6C). After ANG silencing, copper alone presented a decreased effect to stimulate the proliferation of HUVEC cells. However, the ANG knock down was not sufficient to completely inhibit the proliferative action of copper, thus demonstrating that ANG expression is only one of the

several mechanism activated by copper. Interestingly, after selective ANG-knockdown, the presence of the ANG-copper system caused a significant decrease of proliferation versus the protein alone (Fig. 6E-F). Thus, the marked unfavorable effect of copper on proliferative- ANG activity after selective ANG-knockdown, further confirms the negative effect of ANG-copper system on ANG activity.

4. Discussion

In the present work, we reported the effect of copper binding on the biological activity of ANG in endothelial cells. ANG is a member of the secreted ribonuclease family and represents one of the most potent stimulator of angiogenesis. ANG activation induces a wide range of cellular responses (e.g. proliferation, migration effects, promotion of cell survival under stress condition) eventually prompting blood vessels formation.

ANG plays an important role in tumour angiogenesis and it is over-expressed in many cancers. The biological role of ANG should not be limited to induction of angiogenesis. The pivotal role of ANG in neuropathological condition has recently emerged; in fact it is down-regulated in PD and AD (Kim and Kim, 2012) and is one of the key genes in the pathogenesis of ALS (Aparicio-Erriu and Prehn, 2012). Interestingly, the neurovascular degeneration and pathological angiogenesis has recently been related to the onset and progression of different neurodegenerative diseases (Chen, 2013; Kelleher and Soiza, 2013).

The exact etiopathology of almost all neurodegenerative disease (e.g. AD and PD) is still unknown. In parallel with the vascular hypothesis, the pivotal role of metal homeostasis has emerged (e.g. copper, iron, zinc) (Arena, 2012; Jellinger, 2013). Copper dyshomeostasis has been related to the onset and progression of neurodegenerative diseases such as AD (Iakovidis, 2011; Lang, 2013). Copper, at high concentrations, is able to induce angiogenesis. Finney et al. (2007) demonstrated that during HUVECs *in vitro* angiogenesis extracellular translocation of the cytosolic copper occurs. However, to date, the relationship between copper and angiogenesis remains unclear.

It has been reported that the proliferation of endothelial cell is increased in the presence of copper as well as ANG (Hu, 1998a), and metal increases ANG binding to endothelial cells (Soncin, 1997a). Herein, we demonstrate that copper influences different ANG activities in endothelial cells. The experimental setting was complex considering that copper is able to bind ANG (La Mendola, 2010; La Mendola, 2012; Soncin, 1997a) as well as heparin (Raju, 1982), FGF (Shing, 1988) and VEGF (Connolly, 1989). Furthermore, ANG has been related to the VEGF induction of angiogenesis (Kishimoto, 2005) and it is also able to bind heparin (Soncin, 1997b; Yeo, 2014). In order to point out the effect of copper binding on ANG, we investigate the effect of a pre-formed system respect to the protein alone.

By the immunofluorescence assay, we demonstrate that copper binding to ANG is able to modify the intracellular localization of the protein in early stage, blocking the ANG translocation to the nucleus that represents a necessary step for the protein activity. A further confirmation of this effect is the significant decrease of the 45S rRNA transcription induced by the ANG-copper system. Moreover, we reported a sustained activation of intracellular ERK demonstrating that copper

interaction with ANG could increase the permanence of the protein in the membrane or cytosolic compartment. The ANG-copper system affects the protein activity after short time of treatment. In fact, we proved that the binding of copper impairs the migration and angiogenesis induced by ANG in HUVEC cells. Surprisingly, at longer time copper does not affect the proliferative rate of endothelial cells when it is bound to ANG. These diverse temporal effects could be partially explained by the ability of copper to increase the ANG expression in endothelial cells under growth condition. Indeed, it is possible to hypothesize that after copper binds to exogenous ANG, it causes a decrease of the protein effects at short time, thus changing the intracellular trafficking of the protein leading to a decrease of HUVECs migration and angiogenesis. However, at longer time in HUVEC cells a portion of Cu(II) could promote the biogenesis of endogenous ANG contrasting the initial detrimental effect of copper bound to exogenous ANG.

All these findings highlight a close relationship between the metabolic pathways of copper and ANG during the early phase of angiogenic processes. The copper externalization could play a role in the mobilization and internalization of ANG triggering angiogenesis. After that, copper could be re-internalized and exploited its diverse activities.

In conclusion, the mutual influence between copper and ANG could represent a further mechanism underlying the vascular degeneration evidenced in several neurodegenerative pathologies in which alteration of copper metallostasis as well as a decrease of ANG expression is observed.

Conflict of interest statement

None.

Acknowledgements

This work was supported by the PRIN 2010M2JARJ. We thank Rhawnie Caing Carlsson and Daniel Farkas for helpful advice about site-direceted mutagenesis and protein purification. We thank Dr. Simona Daniele for ERK 1/2 phosphorylation assay and analysis of the results.

Figure legends

Fig. 1. Effect of the ANG-copper system on ANG ribonucleolytic activity, ERK 1/2 phosphorylation and 45S gene transcription. (A) Comparative tRNA cleavage activities of ANG at 500 nM, in the presence of increasing amount of Cu(II) equivalent. Each data point represents the mean of at least two experiments performed in duplicate.***P<0.001 vs ANG 0. (B) The time-course of ERK 1/2 phosphorylation in HUVECs by immunoenzymatic assay. (C) HUVECs were treated for 60 min with ANG in the absence or presence of $CuSO_4$ and ERK 1/2 phosphorylation was quantified. The data are expressed as the percentage versus untreated control cells (set to 100%) ± SEM of at three different experiments. *P<0.05; ***P<0.001 vs ANG; ###P<0.001 vs respective $CuSO_4$. (D) One representative Western blot of total ERK and phosphor-ERK in HUVECs after 60 min of treatment with ANG in the presence or absence of $CuSO_4$. (E) Quantitative analysis of the Western blots, performed using ImageJ. Data are expressed as the percentage of OD versus control set to 100% and represent the mean ± SEM of three different experiments. **P<0.01; ***P<0.001 vs ANG; ###P<0.001 vs respective $CuSO_4$. (F) 45S mRNA was quantified by real time RT-PCR. HUVECs were treated with ANG in the absence or in the presence of $CuSO_4$ and Neomycin for 24h. Data are expressed as fold of changes versus basal value (set to 1) and represent the mean ± SEM of three different experiments. *P<0.05, ***P<0.001 vs control; ##P<0.01 vs ANG; §§§P<0.001 vs ANG.

Fig. 2. Intracellular localization of ANG. (A) Representative images of HUVEC cells treated with exogenous ANG in the absence or the presence of $CuSO_4$ for 5-60 min. Sample were fixed and stained with anti-hANG and visualized with goat anti-rabbit AlexaFluo 488 (green). Nuclei were counterstained with DAPI (blue). Two independent experiments were performed in duplicate and five images were taken randomly for each sample. (B) and (C) Mean intensity values of fluorescence measured on the LSM micrographs inside (in) and outside (out) the nuclear areas for HUVEC cell treatments at: 5 min (B) and 60 min (C). Data represent the mean ± SEM of 4–6 randomly chosen fields; *P<0.05, **P<0.001.

Fig. 3. Effect of copper on ANG -induced HUVECs migration. HUVECs were treated with ANG in the absence or in the presence of $CuSO_4$, and healing of the wounds was observed. (A) the average width of the gaps of five scratch wounds, initially at 0h (t_0) and after 8h (t_8) was measured; **P<0.01, ***P<0.001 vs respective average gaps at t_0; (B) the percentage of gap closure; *P<0.05, ***P<0.001 vs control; ##P<0.01, ###P<0.001 vs ANG 100 nM; (C) representative image of

scratch wounds at 0h and 8h. Data represent the mean ± SEM of at least two different experiments performed in triplicate.

Fig. 4. Copper binding on ANG affects angiogenesis in HUVEC cells. Cells were seeded onto Matrigel and treated with ANG in the absence or in the presence of copper. Cells were treated also with ANG nuclear transport inhibitor Neomycin (50 μM) and the H114Y mutant (100 nM) that completely loss the ribonucleolytic activity. Capillary-like tube formation was observed by microscopy after 4h and 16h. (A) The tube length were quantified and expressed as total tube length (μm); (B) the number of branching points were quantified and expressed as a percentage versus the control sample; (C) the number of mesh-like structures were quantified and expressed as a percentage versus the control sample; (D) representative images of HUVECs tube formation after 16h, original magnification was 4×. Data are expressed as the mean ± SEM of two independent experiments performed in triplicate. *P<0.05, **P<0.01, ***P<0.001 vs control; #P<0.05, ##P<0.01, ###P<0.001 vs ANG 100 nM; §§P<0.01, §§§P<0.001 vs ANG 100 nM.

Fig. 5. Copper binding modulation of *in vitro* proliferative and pro-survival effects of ANG in HUVECs. (A) and (B) HUVECs were treated in complete medium with ANG in the absence or presence of different concentration of $CuSO_4$, and the viable cells were counted after 24h (A) or 48h (B) of treatment by MTS assay; (C) HUVECs were treated in serum-withdrawal condition with ANG in the absence or presence of different concentration of $CuSO_4$, and the viable cells were counted after 48h of treatment by MTS assay. Data are expressed as percentage of viable cells respect to control set to 100% and represent the mean ± SEM of three different experiments performed in duplicate. *P<0.05, **P<0.01, ***P<0.001 vs Control; °P<0.05, °°°P<0.001 vs respective $CuSO_4$. (D) Copper induction of ANG gene expression in HUVECs treated with $CuSO_4$ for 24-48h. ANG mRNA was quantified by real time RT-PCR. Data are expressed as fold of changes versus basal value (set to 1) and represented the mean ± SEM of at least three different experiments. **P<0.01, ***P<0.001 vs control.

Fig. 6. Down-regulation of ANG reveals the effect of the pre-formed ANG-copper system on proliferation and pro-survival activity of ANG. HUVECs were treated with control siRNA (CTRL neg) or ANG siRNA before the MTS assay. (A) Efficiency of knock-down was assessed by evaluating the ANG mRNA gene expression by RT-PCR. After electrophoresis separation, densitometric analysis was performed. Data are normalized to β-actin levels, expressed as fold of changes versus control (without siRNA) set to 1 and represented the mean ± SEM of at least three different experiments. ***P<0.001 vs control. (B) Representative image of 2% agarose gel

electrophoresis; (C) HUVECs were treated with increasing concentrations of the ANG in complete medium, and the viable cells were counted after 24-48-72h of treatment by MTS assay; (D) dose-response curve of ANG in complete medium after 24h of treatment (First point = CTRL); (E) and (F) HUVECs were treated in complete medium with ANG in the absence or presence of different concentration of $CuSO_4$, and the viable cells were counted after 24h (E) or 48h (F) of treatment by MTS assay. Data are expressed as percentage of viable cells with respect to control set to 100% and represent the mean ± SEM of three different experiments performed in duplicate. *P<0.05, **P<0.01, ***P<0.001 vs control; #P<0.05, ##P<0.01, ###P<0.001 vs wt-Ang 100 nM; °P<0.05, °°P<0.01 vs respective $CuSO_4$.

References

Aparicio-Erriu IM, Prehn JH. Molecular Mechanisms in Amyotrophic Lateral Sclerosis: The Role of Angiogenin, a Secreted RNase. Front Neurosci 2012; 6:167.

Arena G, Pappalardo G, Sovago I, Rizzarelli E. Copper(II) interaction with amyloid-β: affinity and speciation. Coord Chem Rev 2012; 256: 3-12.

Asada S, Takahashi T, Isodono K, Adachi A, Imoto H, Ogata T, Ueyama T, Matsubara H, Oh H. Downregulation of Dicer expression by serum withdrawal sensitizes human endothelial cells to apoptosis. Am J Physiol Heart Circ Physiol 2008; 295:H2512–21.

Ayton S, Lei P, Bush AI. Metallostasis in Alzheimer's disease. Free Radic Biol Med 2013; 62:76-89.

Badet J, Soncin F, Guitton J-D, Lamare O, Cartwrigth T, Barritault D. Specific binding of angiogenin to calf pulmonary artery endothelial cells. Proc Natl Acad Sci USA 1989; 86:8427-8431.

Cavallucci V, D'Amelio M, Cecconi F. Aβ toxicity in Alzheimer's disease. Mol Neurobiol 2012; 45:366-78.

Chen CC, Chen YC, Hsiao HY, Chang C, Chern Y. Neurovascular abnormalities in brain disorders: highlights with angiogenesis and magnetic resonance imaging studies. J Biomed Sci 2013; 20:47.

Connolly DT, Olander JV, Heuvelman D, Nelson R, Monsell R, Siegel N, Haymore BL, Leimgruber R, Feder J. Human vascular permeability factor. Isolation from U937 cells. J Biol Chem 1989; 264:20017-24.

Crabtree B, Thiyagarajan N, Prior SH, Wilson P, Iyer S, Ferns T, Shapiro R, Brew K, Subramanian V, Acharya KR. Characterization of human angiogenin variants implicated in amyotrophic lateral sclerosis. Biochemistry 2007; 46:11810-8.

D'Andrea LD, Romanelli A, Di Stasi R, Pedone C. Bioinorganic aspects of angiogenesis. Dalton Trans 2010; 39:7625-36.

Del Giudice R, Monti DM, Sarcinelli C, Arciello A, Piccoli R, Hu GF. Amyloidogenic variant of apolipoprotein A-I elicits cellular stress by attenuating the protective activity of angiogenin. Cell Death Dis 2014; 5:e1097.

Drachman DA. The amyloid hypothesis, time to move on: Amyloid is the downstream result, not cause, of Alzheimer's disease. Alzheimers Dement 2014; 10:372-80.

Emara MM, Ivanov P, Hickman T, Dawra N, Tisdale S, Kedersha N, HU GF, Anderson P. Angiogenin-induced tRNA-derived stress-induced RNAs promote stress-induced stress granule assembly. J Biol Chem 2010; 285: 10959-68.

Finney L, Mandava S, Ursos L, Zhang W, Rodi D, Vogt S, Legnini D, Maser J, Ikpatt F, Olopade OI, Glesne D. X-ray fluorescence microscopy reveals large-scale relocalization and extracellular translocation of cellular copper during angiogenesis. Proc Natl Acad Sci U S A 2007; 104:2247-52.

Gao X, Xu Z. Mechanisms of action of angiogenin. Acta Biochim Biophys Sin 2008; 40:619-24.

Greenway MJ, Andersen PM, Russ C, Ennis S, Cashman S, Donaghy C, Patterson V, Swingler R, Kieran D, Prehn J, Morrison KE, Green A, Acharya KR, Brown RH Jr, Hardiman O. ANG mutations segregate with familial and 'sporadic' amyotrophic lateral sclerosis. Nat Genet 2006; 38:411-3.

Hardy JA, Higgins GA. Alzheimer's disease: the amyloid cascade hypothesis. Science 1992; 256:184-5.

Holloway DE, Hares MC, Shapiro R, Subramanian V, Acharya KR. High-level expression of three members of the murine angiogenin family in Escherichia coli and purification of the recombinant proteins. Protein Expr Purif 2001; 22:307-17.

Hu GF, Riordan JF, Vallee BL. Angiogenin promotes invasiveness of cultured endothelial cells by stimulation of cell-associated proteolytic activities. Proc Natl Acad Sci U S A 1994; 91:12096-100.

Hu GF, Riordan JF, Vallee BL. A putative angiogenin receptor in angiogenin-responsive human endothelial cells. Proc Natl Acad Sci U S A 1997; 94:2204-9.

Hu GF. Copper stimulates proliferation of human endothelial cells under culture. J Cell Biochem 1998a; 69:326-35.

Hu GF. Neomycin inhibits angiogenin-induced angiogenesis. Proc Natl Acad Sci U S A 1998b; 95:9791−9795.

Hu GF, Xu CJ, Riordan JF. Human angiogenin is rapidly translocated to the nucleus of human umbilical vein endothelial cells and binds to DNA. J Cell Biochem 2000; 76:452-62.

Iakovidis I, Delimaris I, Piperakis SM. Copper and its complexes in medicine: a biochemical approach. Mol Biol Int 2011; 2011:594529.

Jang SH, Kang DK, Chang SI, Scheraga HA, Shin HC. High level production of bovine angiogenin in E. coli by an efficient refolding procedure. Biotechnol Lett 2004; 26:1501-4.

Jellinger KA. The relevance of metals in the pathophysiology of neurodegeneration, pathological considerations. Int Rev Neurobiol 2013; 110:1-47.

Jimi SI, Ito KI, Kohno K, Ono M, Kuwano M, Itagaki Y, Ishikawa H. Modulation by bovine angiogenin of tubular morphogenesis and expression of plasminogen activator in bovine endothelial cells. Biochem. Biophys. Res Commun 1995; 211:476-83.

Kelleher RJ, Soiza RL. Evidence of endothelial dysfunction in the development of Alzheimer's disease: Is Alzheimer's a vascular disorder?. Am J Cardiovasc Dis 2013; 3:197-226.

Khoo CP, Micklem K, Watt SM. A comparison of methods for quantifying angiogenesis in the Matrigel assay in vitro. Tissue Eng Part C Methods 2011; 17:895-906.

Kieran D, Sebastia J, Greenway MJ, King MA, Connaughton D, Concannon CG, Fenner B, Hardiman O, Prehn JH. Control of motoneuron survival by angiogenin. J Neurosci 2008; 28:14056-61.

Kim YN, Kim DH. Decreased serum angiogenin level in Alzheimer's disease. Prog Neuro-Psychoph 2012; 38:116–120.

Kishimoto K, Liu S, Tsuji T, Olson KA, Hu GF. Endogenous angiogenin in endothelial cells is a general requirement for cell proliferation and angiogenesis. Oncogene 2005; 24:445-56.

La Mendola D, Magrì A, Vagliasindi LI, Hansson Ö, Bonomo RP, Rizzarelli E. Copper(II) complex formation with a linear peptide encompassing the putative cell binding site of angiogenin. Dalton Trans. 2010; 10678-106784.

La Mendola D, Farkas D, Bellia F, Magrì A, Travaglia A, Hansson Ö, Rizzarelli E. Probing the copper(II) binding features of angiogenin. Similarities and differences between a N-terminus peptide fragment and the recombinant human protein. Inorg Chem. 2012; 51:128-41.

Lang M, Fan Q, Wang L, Zheng Y, Xiao G, Wang X, Wang W, Zhong Y, Zhou B. Inhibition of human high-affinity copper importer Ctr1 orthologous in the nervous system of Drosophila ameliorates Aβ42-induced Alzheimer's disease-like symptoms. Neurobiol Aging 2013; 34:2604-12.

Lee FS, Vallee BL. Characterization of ribonucleolytic activity of angiogenin towards tRNA. Biochem. Biophys. Res Commun 1989; 161:121-6.

Li R, Riordan JF, Hu G. Nuclear translocation of human angiogenin in cultured human umbilical artery endothelial cells is microtubule and lysosome independent. Biochem Biophys Res Commun 1997; 238:305-12.

Li S, Hu GF. Emerging role of angiogenin in stress response and cell survival under adverse conditions. J Cell Physiol 2012; 227:2822-6.

Liu S, Yu D, Xu ZP, Riordan JF, Hu GF. Angiogenin activates Erk1/2 in human umbilical vein endothelial cells. Biochem Biophys Res Commun 2001; 287:305-10.

Lyros E, Bakogiannis C, Liu Y, Fassbender K. Molecular links between endothelial dysfunction and neurodegeneration in Alzheimer's disease. Curr Alzheimer Res 2014; 11:18-26.

McAuslan BR, Reilly W. Endothelial cell phagokinesis in response to specific metal ions. Exp Cell Res 1980; 130: 147-57.

Michaelis M, Suhan T, Michaelis UR, Beek K, Rothweiler F, Tausch L, Werz O, Eikel D, Zörnig M, Nau H, Fleming I, Doerr HW, Cinatl J Jr. Valproic acid induces extracellular signal-regulated kinase 1/2 activation and inhibits apoptosis in endothelial cells. Cell Death Differ 2006; 13:446-53.

Milardi D, Rizzarelli E. (Eds.) Neurodegeneration: Metallostasis and Proteostasis. Royal Society of Chemistry, Cambridge, 2011

Miyake M, Goodison S, Lawton A, Gomes-Giacoia E, Rosser CJ. Angiogenin promotes tumoral growth and angiogenesis by regulating matrix metallopeptidase-2 expression via the ERK1/2 pathway. Oncogene. 2014 Feb 24. doi:10.1038/onc.2014.2. [Epub ahead of print]

Narayanan G, Bharathidevi RS, Vuyyuru H, Muthuvel B, Konerirajapuram Natrajan S. CTR1 silencing inhibits angiogenesis by limiting copper entry into endothelial cells. PLoS One 2013; 8:e71982.

Nawaz M, Manzl C, Lacher V, Krumschnabel G. Copper-induced stimulation of extracellular signal-regulated kinase in trout hepatocytes: the role of reactive oxygen species, Ca2+, and cell energetics and the impact of extracellular signal-regulated kinase signaling on apoptosis and necrosis. Toxicol Sci 2006; 92:464-75.

Noda Y, Asada M, Kubota M, Maesako M, Watanabe K, Uemura M, Kihara T, Shimohama S, Takahashi R, Kinoshita A, Uemura K. Copper enhances APP dimerization and promotes Aβ production. Neurosci Lett 2013; 547:10-5.

Nolan T, Hands RE, Bustin SA. Quantification of mRNA using real-time RT-PCR. Nat Protoc 2006; 1:1559-82.

Padhi AK, Kumar H, Vasaikar SV, Jayaram B, Gomes J. Mechanisms of loss of functions of human angiogenin variants implicated in amyotrophic lateral sclerosis. PLoS One 2012; e32479.

Park JH, Lee DW, Park KS. Elevated serum copper and ceruloplasmin levels in Alzheimer's disease. Asia Pac Psychiatry 2014; 6:38-45.

Peña MM, Lee J, Thiele DJ. A delicate balance: homeostatic control of copper uptake and distribution. J Nutr 1999; 129:1251-60.

Pizzo E, Sarcinelli C, Sheng J, Fusco S, Formiggini F, Netti P, Yu W, D'Alessio G, Hu GF. Ribonuclease/angiogenin inhibitor 1 regulates stress-induced subcellular localization of angiogenin to control growth and survival. J Cell Sci 2013; 126:4308-19.

Raju KS, Alessandri G, Ziche M, Gullino PM. Ceruloplasmin, copper ions, and angiogenesis. J Natl Cancer Inst 1982; 69:1183-8.

Sadagopan S, Sharma-Walia N, Veettil MV, Bottero V, Levine R, Vart RJ, Chandran B. Kaposi's sarcoma-associated herpesvirus upregulates angiogenin during infection of human dermal microvascular endothelial cells, which induces 45S rRNA synthesis, antiapoptosis, cell proliferation, migration, and angiogenesis. J Virol 2009; 83:3342-64.

Schafe GE, Swank MW, Rodrigues SM, Debiec J, Doyère V. Phosphorylation of ERK/MAP kinase is required for long-term potentiation in anatomically restricted regions of the lateral amygdala in vivo. Learn Mem 2008; 15:55-62.

Sen CK, Khanna S, Venojarvi M, Trikha P, Ellison EC, Hunt TK, Roy S. Copper-induced vascular endothelial growth factor expression and wound healing. Am J Physiol Heart Circ Physiol 2002; 282:H1821-7.

Sheng J, Yu W, Gao X, Xu Z, Hu GF. Angiogenin stimulates ribosomal RNA transcription by epigenetic activation of the ribosomal DNA promoter. J Cell Physiol 2014; 229:521-9.

Shing Y. Heparin-copper biaffinity chromatography of fibroblast growth factors. J Biol Chem 1988; 263:9059-62.

Soncin F, Guitton JD, Cartwright T, Badet J. Interaction of human angiogenin with copper modulates angiogenin binding to endothelial cells. Biochem Biophys Res Commun 1997a; 236:604-10.

Soncin F, Strydom DJ, Shapiro R. Interaction of heparin with human angiogenin. J Biol Chem 1997b; 272: 9818-24.

Steidinger TU, Standaert DG, Yacoubian TA. A neuroprotective role for angiogenin in models of Parkinson's disease. J Neurochem 2011; 116:334-41.

Subramanian V, Feng Y. A new role for angiogenin in neurite growth and pathfinding: implications for amyotrophic lateral sclerosis. Hum Mol Genet 2007; 16:1445-53.

Tello-Montoliu A, Patel JV, Lip GYH, Angiogenin: a review of the pathophysiology and potential clinical applications. J Thromb Haemost 2006; 4:1864-74.

Tiiman A, Palumaa P, Tõugu V. The missing link in the amyloid cascade of Alzheimer's disease-metal ions. Neurochem Int 2013; 62:367-78.

Wong SK. A 384-well cell-based phospho-ERK assay for dopamine D2 and D3 receptors. Anal Biochem. 2004; 333:265-72.

Wei S, Gao X, Du J, Su J, Xu Z. Angiogenin enhances cell migration by regulating stress fiber assembly and focal adhesion dynamics. PLoS One 2011; 6:e28797.

Wu D, Yu W, Kishikawa H, Folkerth RD, Iafrate AJ, Shen Y, Xin W, Sims K, Hu GF. Angiogenin loss-of-function mutations in amyotrophic lateral sclerosis. Ann Neurol. 2007; 62:609-17.

Yamasaki S, Ivanov P, Hu GF, Anderson P. Angiogenin cleaves tRNA and promotes stress-induced translational repression. J Cell Biol 2009; 185:35-42.

Yang SH, Sharrocks AD, Whitmarsh AJ. MAP kinase signalling cascades and transcriptional regulation. Gene 2013; 513:1-13.

Yeo KJ, Hwang E, Min KM, Jee JG, Lee CK, Hwang KY, Jeon YH, Chang SI, Cheong HK. The dual binding site of angiogenin and its inhibition mechanism: the crystal structure of the rat angiogenin-heparin complex. Chem Commun (Camb) 2014; 50:12966-9.

Yoshioka N, Wang L, Kishimoto K, Tsuji T, Hu GF. A therapeutic target for prostate cancer based on angiogenin-stimulated angiogenesis and cancer cell proliferation. Proc Natl Acad Sci U S A 2006; 103:14519-24.

Fig. 1

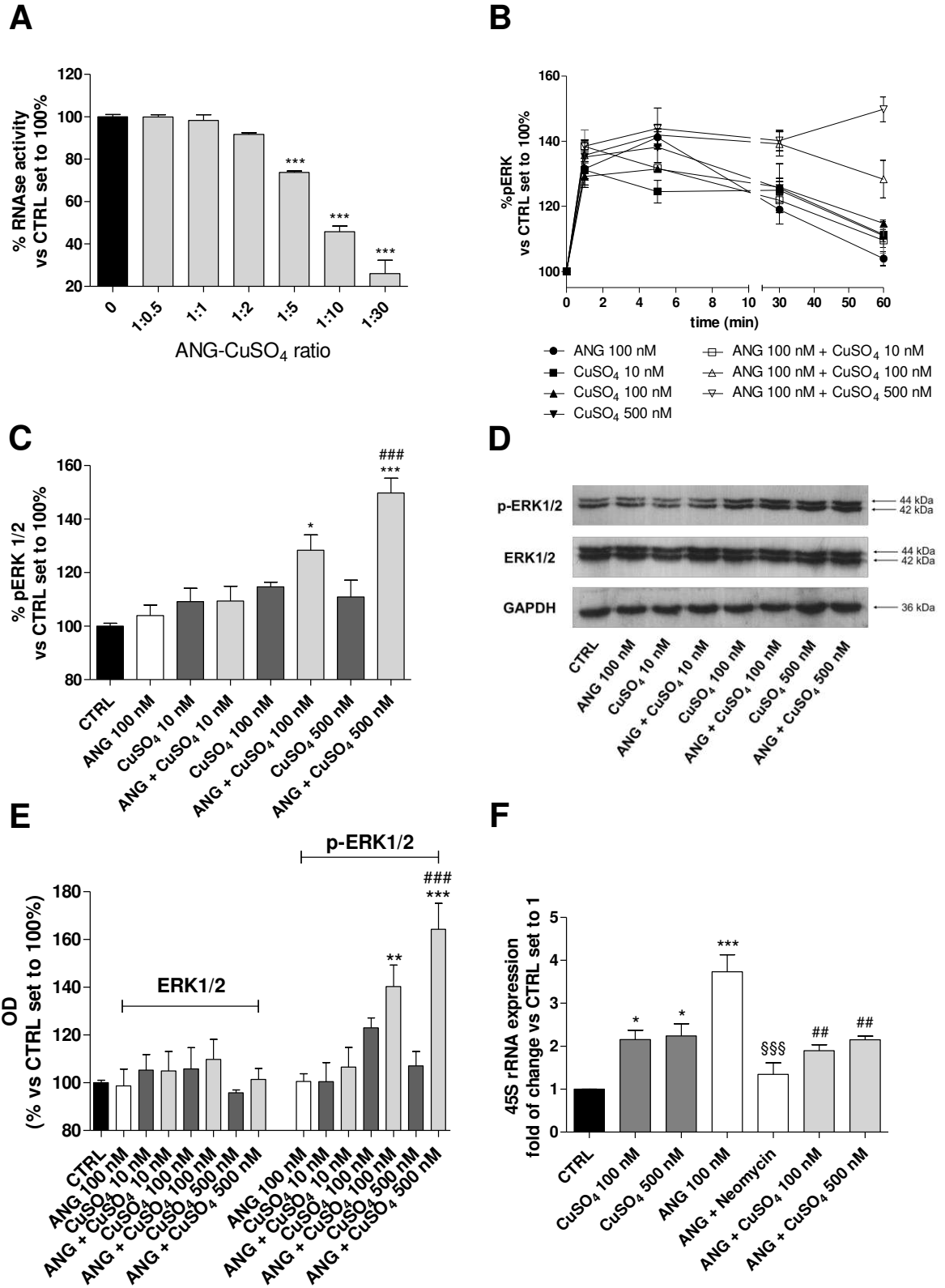
A
% RNAse activity
vs CTRL set to 100%
ANG-CuSO4 ratio
0
1:0.5
1:1
1:2
1:5
1:10
1:30
B
%pERK
vs CTRL set to 100%
time (min)
ANG 100 nM
CuSO4 10 nM
CuSO4 100 nM
CuSO4 500 nM
ANG 100 nM + CuSO4 10 nM
ANG 100 nM + CuSO4 100 nM
ANG 100 nM + CuSO4 500 nM
C
% pERK 1/2
vs CTRL set to 100%
CTRL
ANG 100 nM
CuSO4 10 nM
ANG + CuSO4 10 nM
CuSO4 100 nM
ANG + CuSO4 100 nM
CuSO4 500 nM
ANG + CuSO4 500 nM
D
p-ERK1/2
ERK1/2
GAPDH
44 kDa
42 kDa
36 kDa
E
p-ERK1/2
ERK1/2
OD
(% vs CTRL set to 100%)
F
45S rRNA expression
fold of change vs CTRL set to 1
ANG + Neomycin

Fig. 2

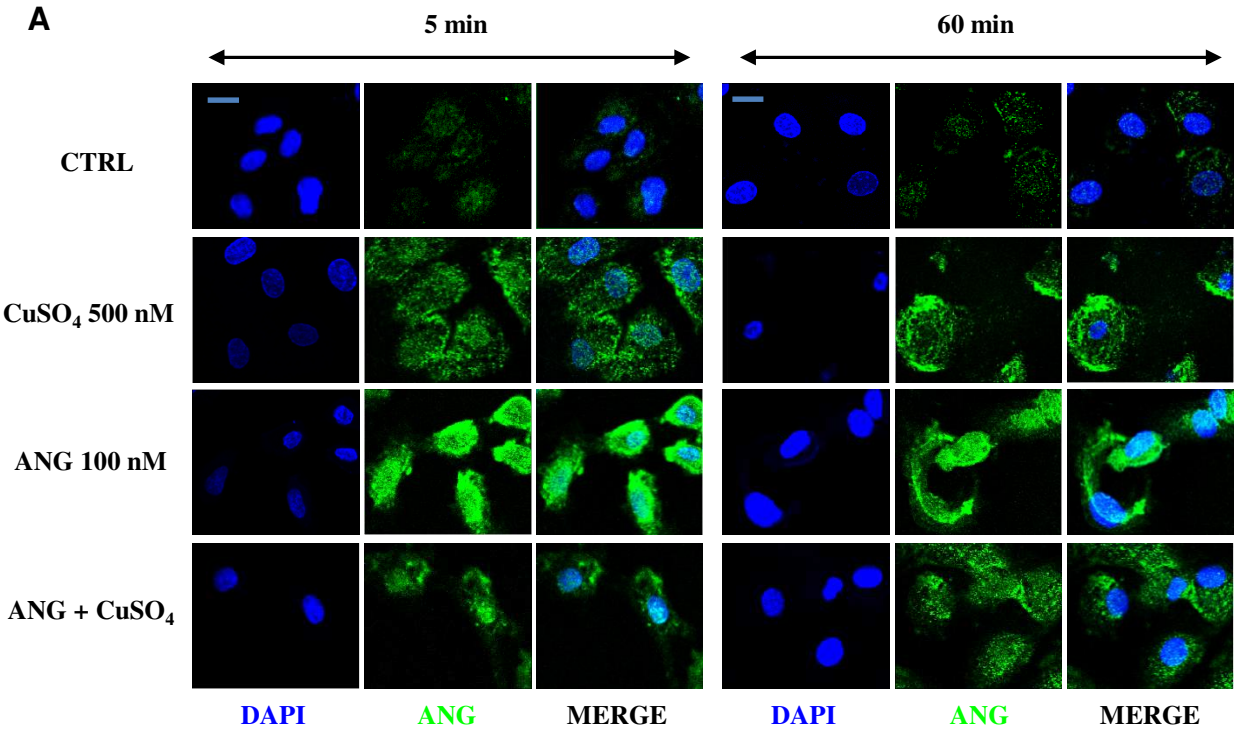
A
5 min
60 min
CTRL
CuSO4 500 nM
ANG 100 nM
ANG + CuSO4
DAPI
ANG
MERGE
DAPI
ANG
MERGE

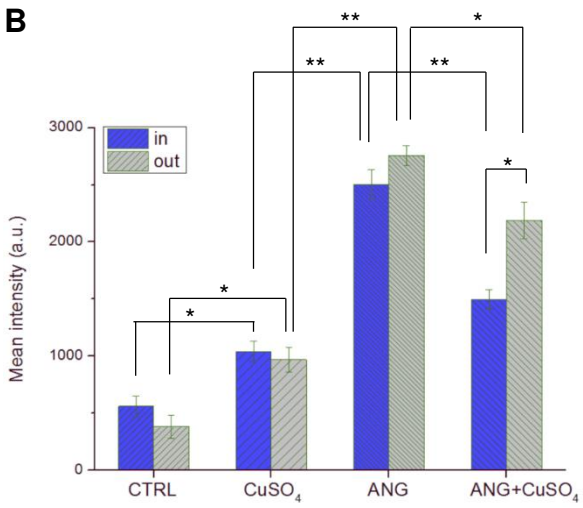
B
Mean intensity (a.u.)
3000
2000
1000
0
in
out
**
**
**
*
*
*
*
CTRL
CuSO4
ANG
ANG+CuSO4

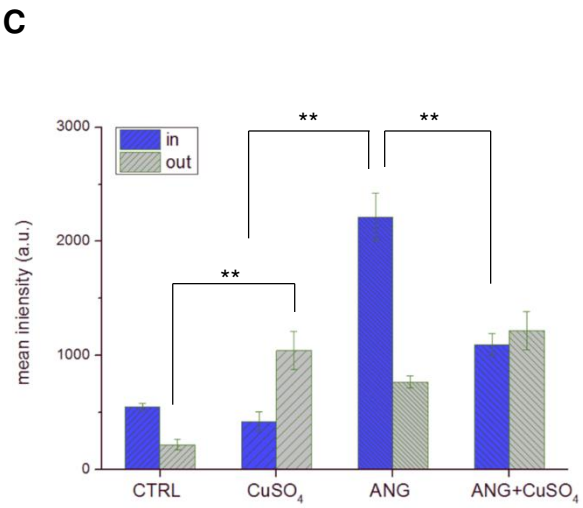
C
mean iniensity (a.u.)
3000
2000
1000
0
in
out
**
**
**
CTRL
CuSO4
ANG
ANG+CuSO4

Fig. 3

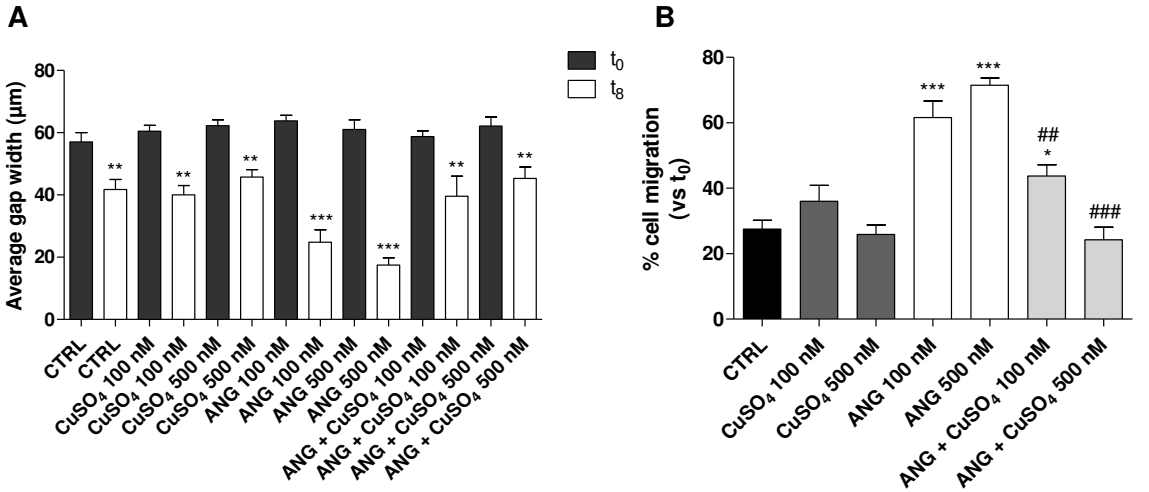
A
Average gap width (µm)
80
60
40
20
0
t_0
t_8
**
**
**
**
***
***
**
**
CTRL
CTRL
$CuSO_4$ 100 nM
$CuSO_4$ 500 nM
ANG 100 nM
ANG 500 nM
ANG + $CuSO_4$ 100 nM
ANG + $CuSO_4$ 500 nM
B
% cell migration (vs t_0)
80
60
40
20
0
***
***
##
*
###
CTRL
$CuSO_4$ 100 nM
$CuSO_4$ 500 nM
ANG 100 nM
ANG 500 nM
ANG + $CuSO_4$ 100 nM
ANG + $CuSO_4$ 500 nM

C

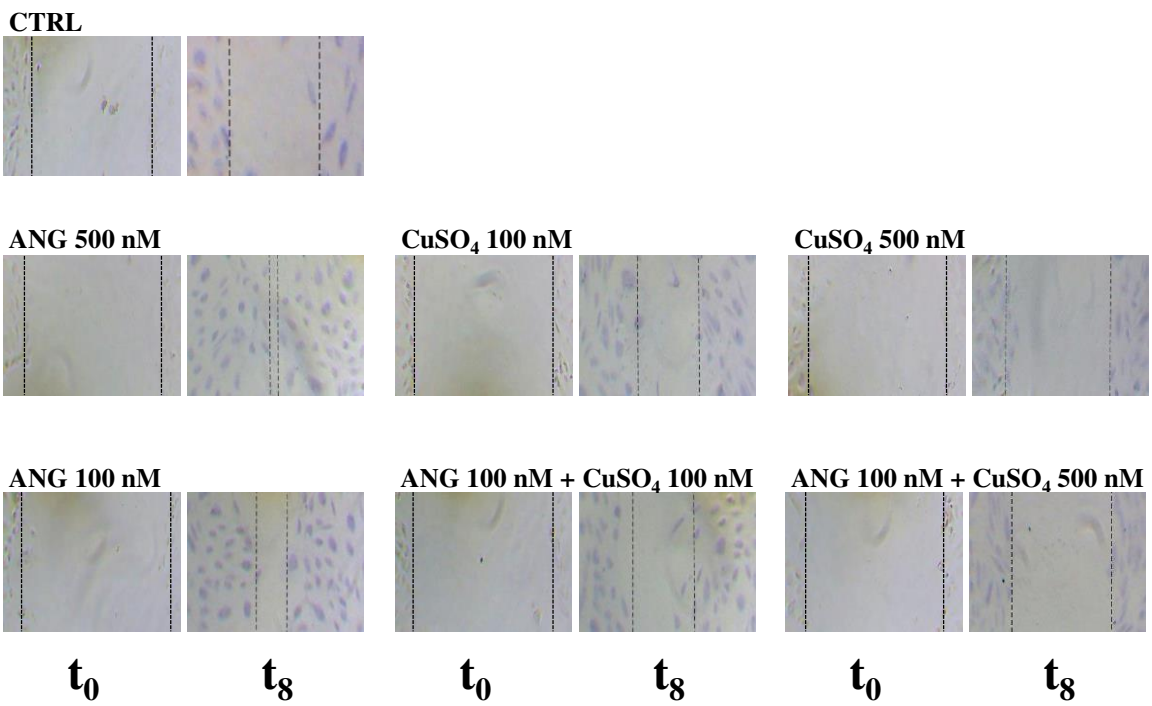
CTRL
ANG 500 nM
$CuSO_4$ 100 nM
$CuSO_4$ 500 nM
ANG 100 nM
ANG 100 nM + $CuSO_4$ 100 nM
ANG 100 nM + $CuSO_4$ 500 nM
t_0
t_8
t_0
t_8
t_0
t_8

Fig. 4

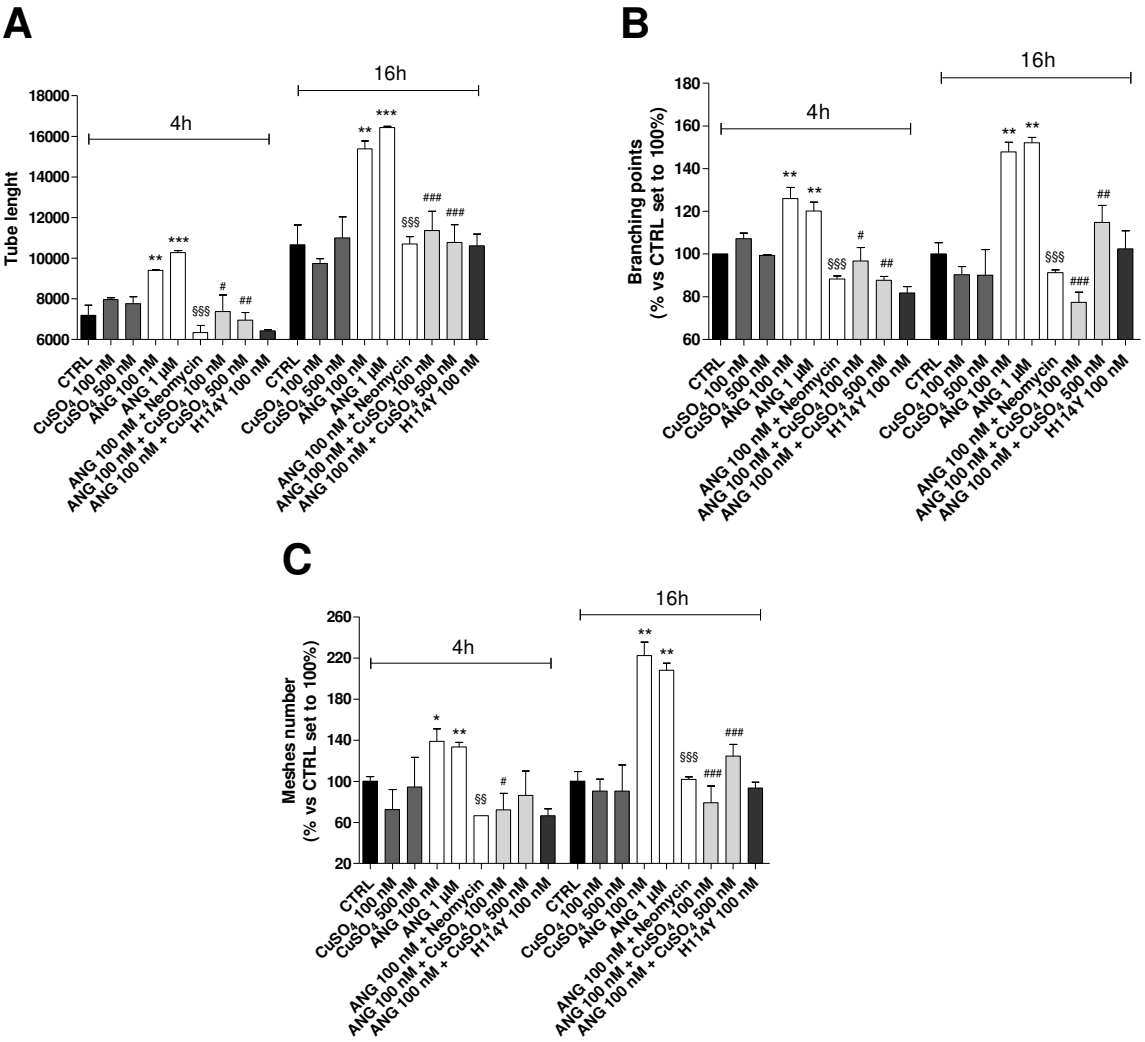
A
B
C
4h
16h
Tube lenght
Branching points
(% vs CTRL set to 100%)
Meshes number
(% vs CTRL set to 100%)
CTRL
100 nM
CuSO4 500 nM
ANG 100 nM
ANG 1 µM
ANG 100 nM + Neomycin
ANG 100 nM + CuSO4 100 nM
ANG 100 nM + CuSO4 500 nM
H114Y 100 nM

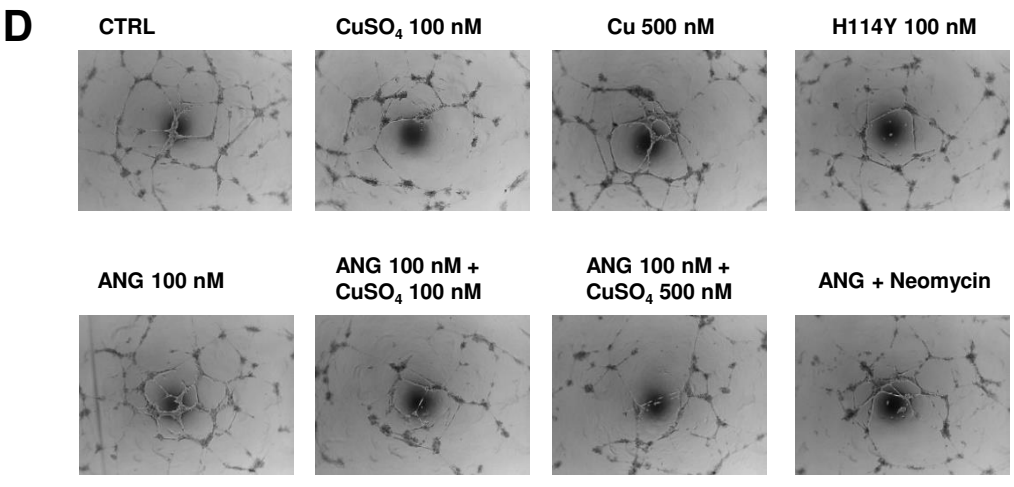
D
CTRL
CuSO4 100 nM
Cu 500 nM
H114Y 100 nM
ANG 100 nM
ANG 100 nM + CuSO4 100 nM
ANG 100 nM + CuSO4 500 nM
ANG + Neomycin

Fig. 5

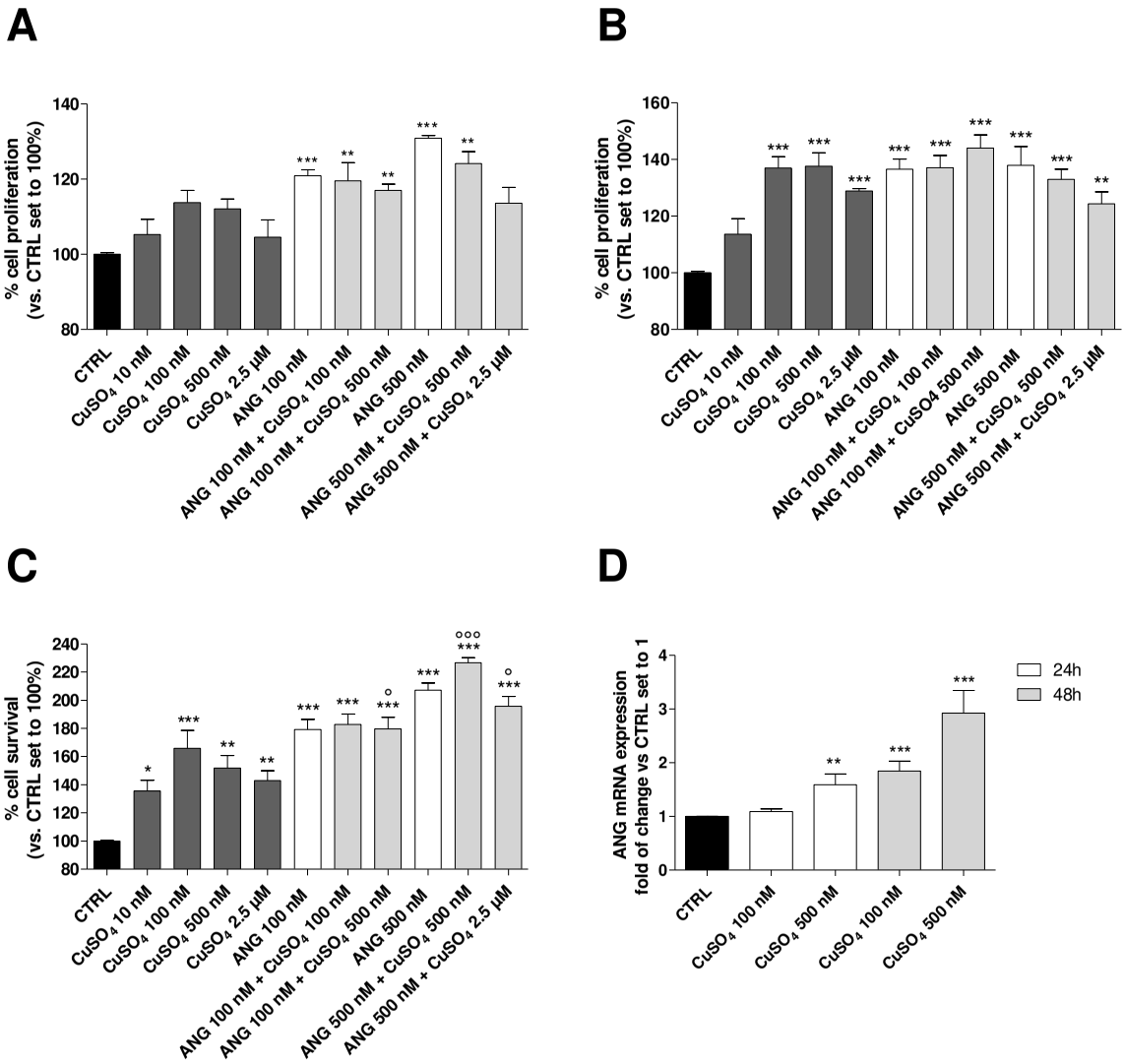
A
% cell proliferation (vs. CTRL set to 100%)
CTRL
CuSO4 10 nM
CuSO4 100 nM
CuSO4 500 nM
CuSO4 2.5 µM
ANG 100 nM
ANG 100 nM + CuSO4 100 nM
ANG 100 nM + CuSO4 500 nM
ANG 500 nM
ANG 500 nM + CuSO4 500 nM
ANG 500 nM + CuSO4 2.5 µM
B
% cell proliferation (vs. CTRL set to 100%)
CTRL
CuSO4 10 nM
CuSO4 100 nM
CuSO4 500 nM
CuSO4 2.5 µM
ANG 100 nM
ANG 100 nM + CuSO4 100 nM
ANG 100 nM + CuSO4 500 nM
ANG 500 nM
ANG 500 nM + CuSO4 500 nM
ANG 500 nM + CuSO4 2.5 µM
C
% cell survival (vs. CTRL set to 100%)
CTRL
CuSO4 10 nM
CuSO4 100 nM
CuSO4 500 nM
CuSO4 2.5 µM
ANG 100 nM
ANG 100 nM + CuSO4 100 nM
ANG 100 nM + CuSO4 500 nM
ANG 500 nM
ANG 500 nM + CuSO4 500 nM
ANG 500 nM + CuSO4 2.5 µM
D
ANG mRNA expression fold of change vs CTRL set to 1
24h
48h
CTRL
CuSO4 100 nM
CuSO4 500 nM
CuSO4 100 nM
CuSO4 500 nM

Fig. 6

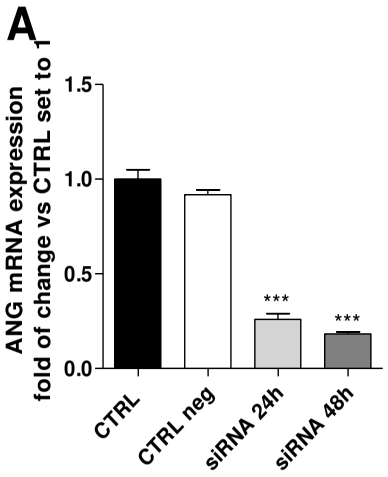
A
ANG mRNA expression
fold of change vs CTRL set to 1
1.5
1.0
0.5
0.0
***
***
CTRL
CTRL neg
siRNA 24h
siRNA 48h

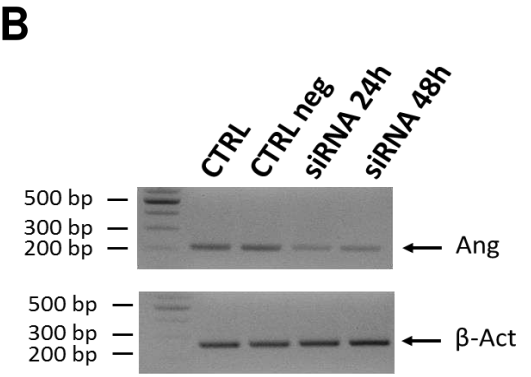
B
CTRL
CTRL neg
siRNA 24h
siRNA 48h
500 bp
300 bp
200 bp
Ang
500 bp
300 bp
200 bp
β-Act

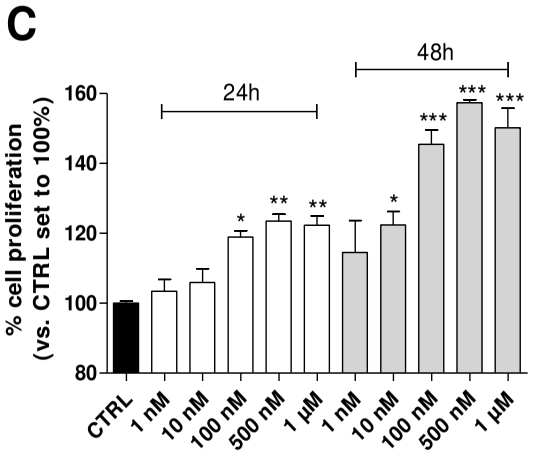
C
% cell proliferation
(vs. CTRL set to 100%)
24h
48h
160
140
120
100
80
*
**
**
*
***
***
***
CTRL
1 nM
10 nM
100 nM
500 nM
1 µM
1 nM
10 nM
100 nM
500 nM
1 µM

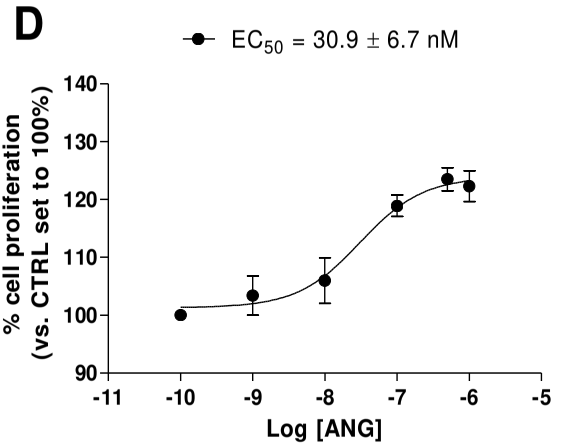
D
EC50 = 30.9 ± 6.7 nM
% cell proliferation
(vs. CTRL set to 100%)
140
130
120
110
100
90
-11
-10
-9
-8
-7
-6
-5
Log [ANG]

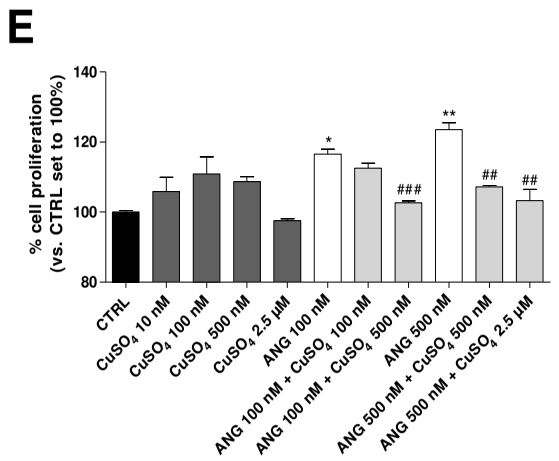
E
% cell proliferation
(vs. CTRL set to 100%)
140
120
100
80
*
**
###
##
##
CTRL
CuSO4 10 nM
CuSO4 100 nM
CuSO4 500 nM
CuSO4 2.5 µM
ANG 100 nM
ANG 100 nM + CuSO4 100 nM
ANG 100 nM + CuSO4 500 nM
ANG 500 nM
ANG 500 nM + CuSO4 500 nM
ANG 500 nM + CuSO4 2.5 µM

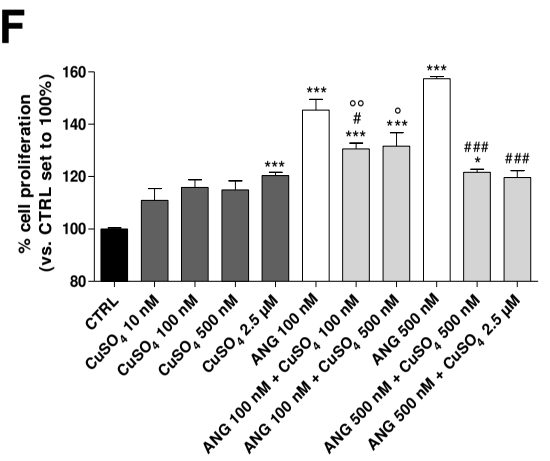
F
% cell proliferation
(vs. CTRL set to 100%)
160
140
120
100
80
***
***
°°
#
***
***
°
***
***
###
*
###
CTRL
CuSO4 10 nM
CuSO4 100 nM
CuSO4 500 nM
CuSO4 2.5 µM
ANG 100 nM
ANG 100 nM + CuSO4 100 nM
ANG 100 nM + CuSO4 500 nM
ANG 500 nM
ANG 500 nM + CuSO4 500 nM
ANG 500 nM + CuSO4 2.5 µM